HYBRIDIZATION EFFECTS IN $CeCoIn_5$ STUDIED BY ANGLE-RESOLVED PHOTOEMISSION SPECTROSCOPY* **

R. Kurleto

Solaris National Synchrotron Radiation Centre, Jagiellonian University
Czerwone Maki 98, 30-392 Kraków, Poland

M. Rosmus

Université Paris-Saclay, CNRS, Institut des Sciences Moléculaires d'Orsay
91405, Orsay, France

Ł. Walczak

PREVAC sp. z o.o., Raciborska 61, 44-362 Rogów, Poland

A. Tejeda

Laboratoire de Physique des Solides, CNRS, Université Paris-Sud
Université Paris-Saclay, 91405 Orsay, France

D. Gnida, D. Kaczorowski

Institute of Low Temperature and Structure Research, Polish Academy of Sciences
P.O. Box 1410, 50-950 Wrocław, Poland

K. Kissner, F. Reinert

Experimentelle Physik VII and Würzburg–Dresden Cluster of Excellence ctd.qmat
Universität Würzburg, Am Hubland, 97074 Würzburg, Germany

P. Starowicz

Marian Smoluchowski Institute of Physics, Jagiellonian University
Łojasiewicza 11, 30-348 Kraków, Poland

Received 26 February 2026, accepted 16 March 2026,
published online 15 May 2026

We studied the electronic structure of a canonical heavy fermion superconductor $CeCoIn_5$ using angle-resolved photoelectron spectroscopy (ARPES). We observed a non-uniform distribution of $4f$-derived spectral weight across the Fermi surface map measured below the coherence temperature ($T =$

* Presented at the Concepts in Strongly Correlated Quantum Matter Conference (CSCQM), Kraków, Poland, 20–22 November, 2025.

** We dedicate this article to Professor Józef Spałek on the occasion of his scientific jubilee.

6 K $< T_{\mathrm{coh}} \approx$ 45 K). Different effects of the coupling between $4f$-states and conduction bands were observed near the Fermi level (E_{F}): *(i)* rapid change of the band slope and increasing $4f$ spectral contribution, when approaching E_{F}, *(ii)* presence of heavy quasiparticle bands ($m^{\star} \sim 100 m_e$).

DOI:10.5506/APhysPolB.57.5-A20

1. Introduction

Here, we present a spectroscopic study of the heavy fermion material $CeCoIn_5$. This class of materials has been an extremely fertile ground for experimental and theoretical studies. Heavy fermion systems are characterized by large effective masses of charge carriers due to strong electronic correlations [1]. Their band structure is strongly renormalized with a spike of density of states (DOS) on the meV scale around the Fermi level (E_{F}). This makes them prone to ground-state instabilities, and one can expect non-trivial phase diagrams with multiple phases including superconductivity.

$CeCoIn_5$ is a system which attracted a lot of attention [1], *i.a.* because of the premise of Fulde–Ferrell–Larkin–Ovchinnikov (FFLO) state [2]. It is a heavy fermion superconductor with a critical temperature $T_{\mathrm{c}} = 2.3$ K and a Sommerfeld coefficient $\gamma = 290$ mJ/(mole$_{\mathrm{Ce}}$ K^2) [3]. According to electrical transport studies, it displays a crossover from the logarithmic Kondo regime to a Fermi liquid below a coherence temperature $T_{\mathrm{coh}} = 45$ K, and subsequently undergoes a transition to superconductivity [3].

Angle-resolved photoelectron spectroscopy (ARPES) is a modern tool for studies of the electronic structure of solids [4]. It has a special place in the research on heavy fermion materials [5], as it can directly visualize heavy quasiparticle bands near the Fermi level (E_{F}) at low temperatures. The experiment can be realized using resonant photoemission by varying photon energy around an absorption edge. This allows us to gain chemical and orbital selectivity in ARPES spectra [6]. The general principle is increasing the population of states near E_{F} by transferring charge carriers from the core level with radiation tuned to the resonance energy. However, multiple configurations in the final state appear (Fig. 1 (a)) and the photoemission spectrum is a result of quantum interference between different channels such as: Auger process, spectator or participant decay. We provide a more detailed description specific to Ce intermetallics in the next section.

In this paper, we identify hybridization effects in the electronic structure of $CeCoIn_5$ using ARPES at the Ce $4d$–$4f$ resonance. We observe how free-electron-like parabolic bands are getting flat close to the Fermi level. We interpret this behavior using the Kondo band mixing model, which allows us to obtain quantitative characteristics: the position of $4f$ level (ε_f) with

respect to E_F and hybridization strength (V). Moreover, we present heavy fermion dispersions found in a different region of the Brillouin zone. These results complement our previous studies on $CeCoIn_5$, where we reported on the formation of electronic bands with large effective masses $m^\star \sim 100 m_e$ [7].

2. Experimental

ARPES measurements of $CeCoIn_5$ were performed at CASSIOPEE beamline (Soleil, France) using the Scienta R4000 analyser. Flux-grown samples were cleaved *in situ* along (001) plane in the ultra-high vacuum (UHV) setup with a base pressure of $p \approx 10^{-11}$ mbar. All spectra were recorded at temperature equal to 6 K, and using linear horizontal polarization of incident radiation. Photon energy corresponding to the Ce $4d$–$4f$ resonant transition ($h\nu = 122$ eV) was used to enhance photoemission from Ce $4f$ states. Off-resonance measurements were taken at $h\nu = 80$ eV. The total instrumental resolution was better than 18 meV. Other data collected on the same sample were published before [7].

3. Results

3.1. Resonant photoemission studies of Ce compounds

Resonant photoelectron spectroscopy, generally outlined in Fig. 1, applied to Ce intermetallics focuses on two resonant transitions: $4d$–$4f$ at photon energy $h\nu \approx 122$ eV and $3d$–$4f$ at $h\nu \approx 882$ eV, where exact values of photon energy depend on the studied material. Systematic changes of the photoemission spectrum when the photon energy is scanned across the Ce $4d$–$4f$ resonance are well exemplified for another system, namely $Ce_2Co_{0.8}Si_{3.2}$ (Fig. 1 (b)), which has been studied before [8, 9]. Off-resonance spectra ($h\nu < 118$ eV) are consistently showing a hump centered around -1 eV and no special features at E_F. On-resonance spectra ($h\nu \geq 118$ eV) have a radically different shape with elevated intensity near E_F and a broad peak at around 2 eV. The near-E_F signal is maximal at $h\nu = 122$ eV (resonance transition energy) and consists of two narrower peaks. The same features are visible in the spectra of $CeCoIn_5$ (presented also in k-resolved form, Fig. 1 (c1) and (c2)), as they are characteristic of Ce intermetallics. The universal features of the low-temperature Ce $4f$ photoemission spectrum can be explained qualitatively on the basis of single impurity Anderson model (SIAM) [10, 11]. Each peak corresponds to a photoemission final state with a certain number of electrons on a given f level, and they are characterized by different screening levels of a created hole (Fig. 1 (d)). The broad f^0 peak corresponds to an empty $4f$ subshell in a final state of photoemission, whereas $f^1_{7/2}$ and $f^1_{5/2}$ peaks are related to one electron in either $f_{7/2}$ or $f_{5/2}$ final state, respectively. In particular, the latter peak, located close to

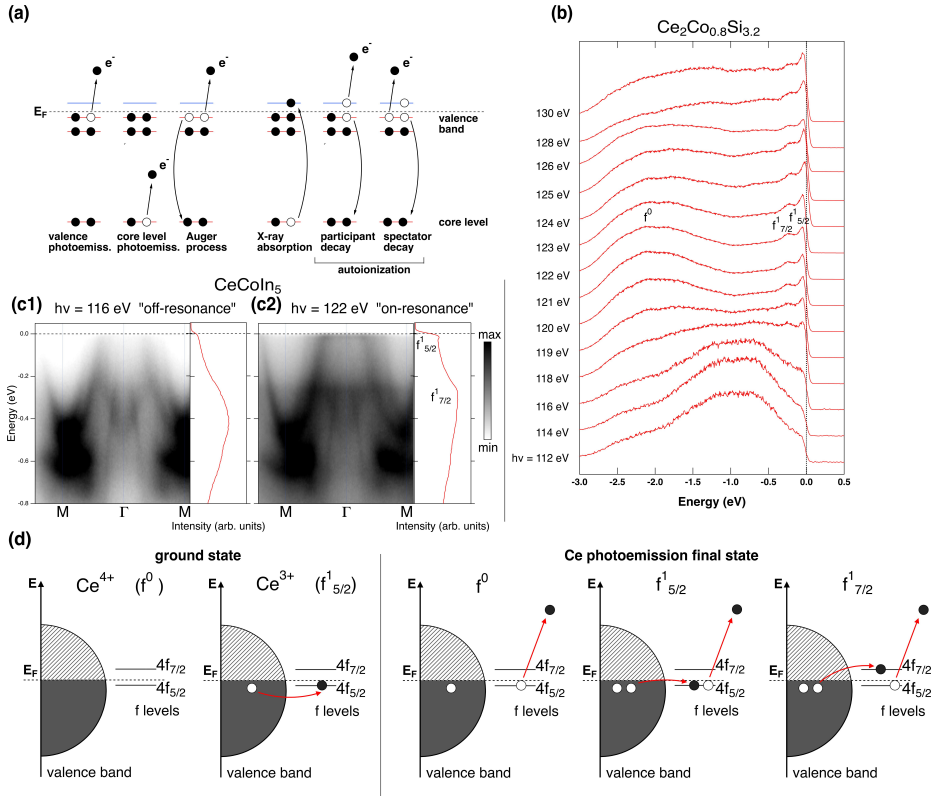

Fig. 1. Resonance photoelectron spectroscopy. (a) Schematic illustration showing different excitation–deexcitation processes in general (starting from the left): direct valence band photoemission, core level photoemission, Auger process, X-ray absorption, participant and spectator decay [6]. (b) Resonance photoelectron spectroscopy data for $Ce_2Co_{0.8}Si_{3.2}$ obtained at the Ce $4d$–$4f$ absorption edge (own results). The spectra were collected at $T = 100$. (c1) "off-resonance" ARPES spectrum ($h\nu = 116$ eV) for $CeCoIn_5$ collected at $T = 6$ K. (c2) "on-resonance" ARPES spectrum ($h\nu = 122$ eV) for $CeCoIn_5$ collected at $T = 6$ K. For both (c1) and (c2) a curve resulting from angle integration is provided. (d) Schematic presentation of ground state and photoemission final states characteristic of Ce intermetallics. We ignore the crystal electric field (CEF) splitting, because it is not resolved in our experimental data.

E_F, is particularly sharp. These final states appear as a result of photoemission from a ground state, which is a combination of two configurations: $Ce^{4+}(f^0)$ and $Ce^{3+}(f^1)$. The different configurations, both in final states and the ground state, are present due to finite hybridization V between the $4f$ level and the valence band. On-resonance photon energy ($h\nu = 122$ eV) was also used to obtain the Fermi surface map shown in Fig. 2.

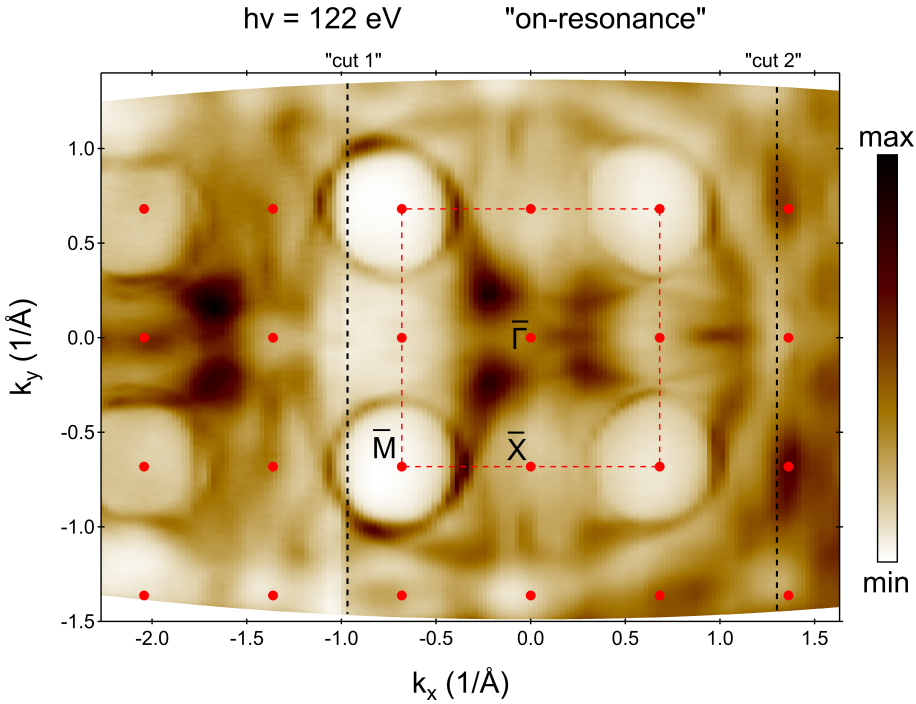

Fig. 2. Fermi surface map of $CeCoIn_5$ measured at the Ce $4d$–$4f$ resonance ($h\nu =$ 122 eV) well below the coherence temperature ($T = 6$ K) [7]. High symmetry points (red markers) and the BZ contour (red dashed line) are indicated. "cut 1" and "cut 2" refer to band structure sections analyzed further in the manuscript.

3.2. Dispersion modification due to c–f hybridization

Change in the dispersion character near E_F can be described by the Kondo mixing model. Here, we consider a single band hybridizing with one level from the entire f-electron crystal field manifold. Then, the renormalized dispersion has two branches $\tilde{\varepsilon}_\pm$, given by the formula

$$\tilde{\varepsilon}_\pm = \frac{\varepsilon_c + \varepsilon_f}{2} \pm \frac{1}{2}\sqrt{(\varepsilon_c - \varepsilon_f)^2 + 4|V|^2}\,, \tag{3.1}$$

where ε_f denotes the position of the f-electron level, ε_c is an input conduction band dispersion, and V is a mixing strength measure (hybridization parameter). Renormalized dispersion generated for realistic values of parameters is shown in Fig. 3 (a1), (a2) (black lines), with projected contributions of non-f states ((a1), blue) and f states ((a2), red) (marker size is proportional to a given contribution). The band is getting flatter and gaining more

f-electron character when approaching the position of the original atomic-like f level (indicated by the red dashed line). Far from the original f-level position, the dispersion is close to the input conduction band dispersion (indicated by the blue dashed line).

Experimental evidence of hybridization effects for the case of $CeCoIn_5$ is also presented in Fig. 3. We analyze the on-resonance spectrum collected at $k_x = -0.97$ 1/Å ("cut 1" indicated in Fig. 2). Raw data (b) already show the change in the slope of the band close to E_F. However, the flattest part of the band is present in the thermally populated part of the spectrum above E_F, which is visible better after performing the maximal angular contrast procedure (MAC) [12] (c) or division by the Fermi function (d). The processed and raw data consistently show the peak at E_F in integrated EDC (energy distribution curve) (e) due to the presence of the flat band.

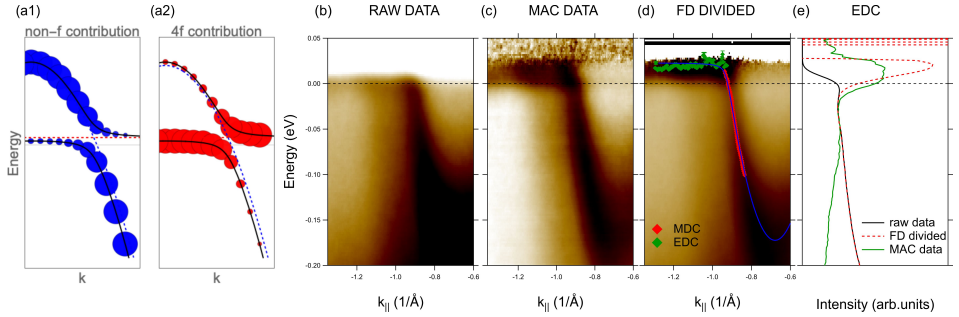

Fig. 3. Effect of hybridization between $4f$ level and the conduction band in $CeCoIn_5$. Rapid change in band dispersion according to the Kondo mixing model is shown schematically in (a1) and (a2). Band composition is indicated by the marker size on two separate panels (blue for original conduction band contribution in panel (a1), red for f-orbital in panel (a2)). (b) Experimental observation of $4f$ — conduction band hybridization in the spectrum measured under $4d$–$4f$ resonance conditions ($h\nu = 122$ eV) along "cut 1" (see Fig. 2) for $CeCoIn_5$ at $T = 6$ K, which is well below the coherence temperature. (c) The same data but in a contrast-enhanced version (MAC procedure applied [12]). (d) The same spectrum divided by the Fermi function. Markers indicate EDC (green) and MDC (red) maxima derived from Lorentzian fits. The Kondo mixing model fit is indicated by the blue line. (e) EDCs integrated in k-range between 0.8 and 1.3 1/Å using data shown in (b)–(d). All curves show consistently a peak related to the $4f$-derived flat band near E_F.

To quantify the effects of hybridization, we neglected the dispersion of the original f level (*i.e.*, $\varepsilon_f =$ const.) and used a parabolic dispersion for the input conduction band

$$\varepsilon_c = \varepsilon_0 + \frac{\hbar^2 k^2}{2m^\star}\,, \tag{3.2}$$

where ε_0 is a conduction band minimum and $m^\star$ is an effective mass. Then we fitted the lower branch (ε_-) of the model given by Eq. (3.1) to MDC (momentum distribution curve) and EDC-derived maxima. According to the fit, the original $4f$-level is located at $\varepsilon_f = 23$ meV above E_F and the hybridization strength is equal to $V = 17(1)$ meV. The input conduction band has a bottom located at $\varepsilon_0 = -171(1)$ meV, and it is characterized by the effective mass $m^\star = 1.2m_e$. Other values could be found for different locations in BZ, especially since anisotropic and band-dependent hybridization effects have been observed for $CeCoIn_5$ [7, 13]. Similar analysis of $4f$-derived band dispersion has been performed for the case of $CeCoGe_{1.2}Si_{0.8}$ [14].

3.3. Heavy electron mass behavior around the X point

Another aspect of the hybridization between the conduction band and Ce $4f$ electrons is that it leads to the formation of heavy fermion bands. In the previous study [7], we succeeded in tracing heavy band dispersion in the ARPES data obtained at $T = 6$ K, and the resulting effective masses ranged from 30 to 130 free electron mass. One of the paths in k-space with a visible heavy band crossed $\bar{X}$ points along the $\bar{X}$–$\bar{\Gamma}$–$\bar{X}$ path. Here, we present a heavy band located near the $\bar{X}$–$\bar{\Gamma}$–$\bar{X}$ path but obtained in other experimental geometry (with respect to that in Ref. [7]), namely along "cut 2" shown in Fig. 2. The f-electron dispersion is presented in Fig. 4. The Fermi function normalization revealed its actual position above E_F and parabolic fits yielded effective masses equal to $210m_e$ and $80m_e$ as shown in Fig. 4 (b). ARPES has the ability to determine effective masses locally, but their average effect is reflected in global parameters. For example, such masses generally agree with the Sommerfeld coefficient for $CeCoIn_5$, which equals $\gamma = 290$ mJ/(mole$_\mathrm{Ce}$ K^2) [3]. They also agree with the effective masses of the order of $100m_e$ revealed by the quantum oscillation experiments [15]. Significant mass renormalization of similar order was also found in infrared studies of $CeCoIn_5$ [16]. The obtained effective masses are close to our earlier estimates of $130m_e$ and $86m_e$ derived from fits crossing the $\bar{X}$ points, *i.e.* at a slightly different position in k-space. One can notice a difference between dispersions obtained for negative and positive k_y values, although these regions are equivalent in k-space. Possible explanations of this fact can be related to experimental geometry. First, a photoemission at positive and negative k_y is characterized by different matrix element effects, hence bands of different orbital characters can be probed. Second, even a slight misalignment of the sample can result in observation of different dispersions on both sides of Fig. 4.

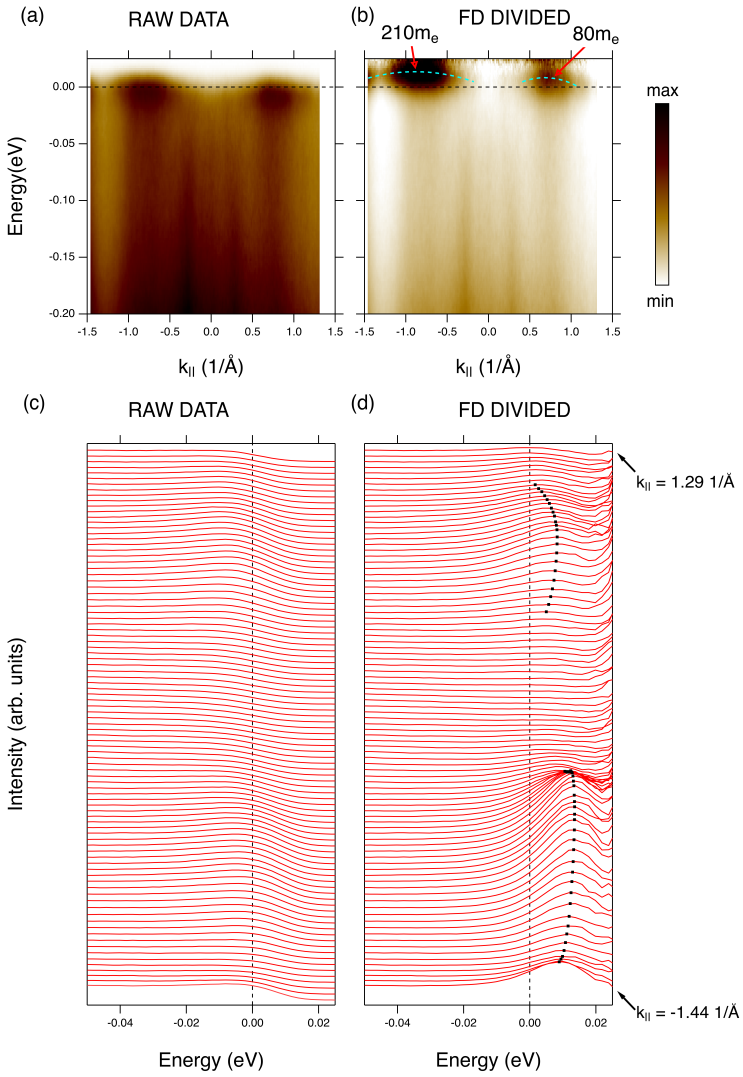

Fig. 4. Visualization of heavy bands just above the Fermi level along "cut 2" in the Fig. 2, obtained with photon energy $h\nu = 122$ eV at temperature $T = 6$ K. The raw data collected close to the Γ–X line ($k_x = 1.3$ 1/Å) show enhanced intensity at the E_F as visible in the color scale representation (a) and in the waterfall (c). Hole pockets with the masses $\sim 100m_e$ are recovered after dividing by the Fermi function as visible in the color scale representation (b) and in the waterfall (d). Peak maxima are indicated by black dots on the waterfall (d), and cyan dashed lines on spectrum (b) indicate the maxima of fitted parabolas.

4. Conclusions

The ARPES studies of $CeCoIn_5$ revealed distinct effects of the hybridization between valence band and f-electrons in a vicinity of E_F. We observed how the almost free electron band ($m^\star = 1.2m_e$) is getting flat on a scale of 20 meV around the Fermi level, which is a unique and truly amazing feature of heavy fermion materials. Some sections of the near E_F $4f$-derived band structure are dispersive with the large effective mass ($m^\star \sim$ 80–$200m_e$), which is consistent with the specific heat data, quantum oscillation experiments, and infrared studies of $CeCoIn_5$.

First, we would like to express our gratitude to Professor Józef Spałek for past and ongoing collaboration and fruitful discussions, which have a stimulating effect on our research into heavy fermion systems and other materials with strong electronic correlations. We acknowledge Synchrotron Soleil (France) SOLEIL for the provision of synchrotron radiation facilities and we would like to thank J.E. Rault and F. Bertran for their assistance in using beamline CASSIOPEE under proposal 20160235. Experimental data presented in this paper were obtained thanks to the financial support of the National Science Centre (NCN), Poland, within grants No. 2016/23/N/ST3/02012 and No. 2015/19/B/ST3/03158.

REFERENCES

[1] P. Coleman, «Heavy Fermions: Electrons at the Edge of Magnetism», in: «Handbook of Magnetism and Advanced Magnetic Materials», *Wiley*, 2007.

[2] A. Bianchi *et al.*, «Possible Fulde–Ferrell–Larkin–Ovchinnikov Superconducting State in $CeCoIn_5$», *Phys. Rev. Lett.* **91**, 187004 (2003).

[3] C. Petrovic *et al.*, «Heavy-fermion superconductivity in $CeCoIn_5$ at 2.3 K», *J. Phys.: Condens. Matter* **13**, L337 (2001).

[4] J.A. Sobota, Y. He, Z.-X. Shen, «Angle-resolved photoemission studies of quantum materials», *Rev. Mod. Phys.* **93**, 025006 (2021).

[5] S.-i. Fujimori, «Band structures of $4f$ and $5f$ materials studied by angle-resolved photoelectron spectroscopy», *J. Phys.: Condens. Matter* **28**, 153002 (2016).

[6] P.A. Brühwiler, O. Karis, N. Mårtensson, «Charge-transfer dynamics studied using resonant core spectroscopies», *Rev. Mod. Phys.* **74**, 703 (2002).

[7] R. Kurleto *et al.*, «Photoemission signature of momentum-dependent hybridization in $CeCoIn_5$», *Phys. Rev. B* **104**, 125104 (2021).

[8] P. Starowicz *et al.*, «Evidence of momentum-dependent hybridization in $Ce_2Co_{0.8}Si_{3.2}$», *Phys. Rev. B* **89**, 115122 (2014).

[9] P. Starowicz *et al.*, «Valence Band of $Ce_2Co_{0.8}Si_{3.2}$ and Ce_2RhSi_3 Studied by Resonant Photoemission Spectroscopy and FPLO Calculations», *Acta Phys. Pol. A* **126**, A-144 (2014).

[10] A. Sekiyama *et al.*, «Probing bulk states of correlated electron systems by high-resolution resonance photoemission», *Nature* **403**, 396 (2000).

[11] S. Patil, G. Adhikary, G. Balakrishnan, K. Maiti, «Unusual spectral renormalization in hexaborides», *J. Phys.: Condens. Matter* **23**, 495601 (2011).

[12] T. Greber, T.J. Kreutz, J. Osterwalder, «Photoemission above the Fermi Level: The Top of the Minority d Band in Nickel», *Phys. Rev. Lett.* **79**, 4465 (1997).

[13] A. Koitzsch *et al.*, «Band-dependent emergence of heavy quasiparticles in $CeCoIn_5$», *Phys. Rev. B* **88**, 035124 (2013).

[14] H.J. Im *et al.*, «Direct Observation of Dispersive Kondo Resonance Peaks in a Heavy-Fermion System», *Phys. Rev. Lett.* **100**, 176402 (2008).

[15] J. Hornung *et al.*, «Anomalous quantum oscillations of $CeCoIn_5$ in high magnetic fields», *Phys. Rev. B* **104**, 235155 (2021).

[16] M. Lee *et al.*, «Temperature-dependent f-electron evolution in $CeCoIn_5$ via a comparative infrared study with $LaCoIn_5$», *Results Phys.* **47**, 106376 (2023).